Gabor Filtering of Complex Hue/Saturation Images for Color Texture Classification

Christoph Palm, Daniel Keysers, Thomas Lehmann, Klaus Spitzer

Institute of Medical Informatics
Aachen University of Technology (RWTH)
52074 Aachen, Germany,

Email: cpalm@mi.rwth-aachen.de

Abstract

Objective: Complex hue/saturation images as a new approach for color texture classification using Gabor filters are introduced and compared with common techniques.
Method: The interpretation of hue and saturation as polar coordinates allows direct use of the HSV-colorspace for Fourier transform. This technique is applied for Gabor feature extraction of color textures. In contrast to other color features based on the RGB-colorspace [1] the combination of color bands is done previous to the filtering.
Results: The performance of the new HS-features is compared with that of RGB based as well as grayscale Gabor features by evaluating the classification of 30 natural textures. The new HS-features show same results like the best RGB features but allow a more compact representation. On the average the color features improve the results of grayscale features.
Conclusion: The consideration of the color information enhances the classification of color texture. The choice of colorspace cannot be adjudged finally, but the introduced features suggest the use of the HSV-colorspace with less features than RGB.

1 Introduction

Texture is an important aspect of image analysis for classification and segmentation as well as image generation, computer vision, graphics and image processing. In the last thirty years a large number of algorithms for texture feature extraction have been developed. Statistical algorithms describe classes of similar textures. Differences in one class are accredited to an underlying stochastic process. Prominent representatives for statistical texture feature extraction methods are Gauss-Markov-Random-Fields [2], Co-Occurrence-Matrices [3] as well as Gabor- and Wavelet-representations [4, 5]. The reason for the multitude of features for texture analysis is the lack of complete understanding and description of textures up to now. Therefore the ideal feature set has to be determined for a specific application.

Although real-world scenes are colored, most of the research has been done in the field of grayscale textures. Reasons for that were high costs for color cameras, high computational costs for color image processing, and the large complexity even of grayscale textures. In the past few years the first steps were done in recognition of colored textures. This results from decreasing hardware costs and the variety of features in the grayscale domain. The migration of methods from grayscale to color images is diffi-

cult because of the transition from scalars to vectors which involves the loss of order-relation. A simple sequential analysis of the three color bands red, green and blue entails the problem of merging the results and disregarding the correlation between the color bands. However, color texture features based on Wavelets [6], Gabor filters [1], Co-Occurrence [7] and Auto-Covariance [8] were recently presented.

This paper focuses on Gabor filters for colored textures. Beside the method of JAIN [1], which is based on the RGB-colorspace (*R*ed, *G*reen, *B*lue), a new method working with the HSV-colorspace (*H*ue, *S*aturation, *V*alue) is presented. Hue and Saturation are represented as complex valued images, which was introduced by FREY [9]. This sight on color now is proposed especially for Fourier-based texture feature extraction methods like Gabor filters. By combination of nonlinear color transform and texture feature extraction excellent classification results of real-world textures can be achieved.

2 Grayscale Gabor Filters

In this section the 2D-Gabor filters and their application to feature extraction of grayscale textures are described. After the introduction of continous 2D–Gabor filters, the discrete Gabor decomposition of the Fourier plane is derived, resulting in grayscale Gabor features.

2.1 2D–Gabor Filters

Frequency elements are important features for texture description. To deal with non-stationary images the local frequencies of small image regions can be analysed by the WFT (*W*indowed *F*ourier *T*ransform) (1), which gives a spatial/frequency representation of the image. For that purpose the 2D continous image $p(x, y)$ is multiplied by the window function $q(x, y)$, followed by the Fourier transform.

$$\begin{aligned} & W(x_0, y_0, u, v) \qquad (1) \\ = & \int_{-\infty}^{\infty} p(x,y) q(x - x_0, y - y_0) e^{-2\pi i(ux+vy)} dxdy \end{aligned}$$

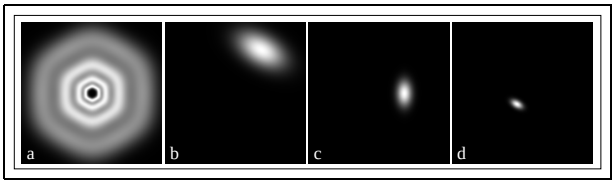

Figure 1: (a) Gabor filter bank (frequency domain) for 6 orientations and 4 center frequencies. (b-d) $M_{f,\varphi}(u, v)$ with $\varphi = 5.24$, $f = 90.51$; $\varphi = 2.09$, $f = 22.63$; $\varphi = 0$, $f = 45.26$.

$$\begin{aligned} = & e^{-2\pi i(ux_0+vy_0)} \\ & \left[p(x_0, y_0) * \left(q(x_0, y_0) e^{2\pi i(ux_0+vy_0)}\right)\right] \\ = & e^{-2\pi i(ux_0+vy_0)} \left[p(x_0, y_0) * m_{u,v}(x_0, y_0)\right] \qquad (2) \end{aligned}$$

where u, v are the horizontal and vertical frequencies, respectively, and (x_0, y_0) is the image location where the frequencies are determined. Equation 2 shows the WFT as a convolution of the image with the filter $m_{u,v}(x, y)$, which is the complex sinusoidal modulated window function for fixed frequencies (u, v). For texture analysis both spatial and frequency locations are desired. With respect to the uncertainty principle a compromise between these two goals has to be found. GABOR [10] used the Gaussian function as the optimally concentrated function in the spatial and in the frequency domain. For non-isotropic Gaussians two new parameters have to be introduced [11]: the aspect ratio $1/\lambda$ and the orientation angel φ of the minor axis to the u-axis. If the Gaussian window and the complex sine are assumed to be equally rotated, the Gabor filter has the form

$$m_{f,\varphi}(x, y) = \frac{1}{2\pi\sigma^2\lambda} e^{-\frac{1}{2}\frac{x'^2/\lambda^2 + y'^2}{\sigma^2}} e^{2\pi i f x'} \qquad (3)$$

$$M_{f,\varphi}(u, v) = e^{-2\pi^2\sigma^2[(u'-f)^2\lambda^2 + v'^2]} \qquad (4)$$

with the center frequency $f = \sqrt{u_0^2 + v_0^2}$ and the rotated coordinates

$$(x', y') = (x\cos\varphi + y\sin\varphi, -x\sin\varphi + y\cos\varphi), \qquad (5)$$

(u', v') analogue. Caused by the convolution theorem and suppression of the factor in (2) the filter interpretation of the Gabor transform allows the efficient computation of the Gabor coefficients $g_{f,\varphi}(x, y)$ (6). After multiplication of the Fourier transform of

the image $P(u,v)$ with that of the Gabor filter (4), $M_{f,\varphi}(u,v)$, the inverse (fast) Fourier transform FFT is applied

$$g_{f,\varphi}(x,y) = \mathrm{FFT}^{-1}\Big\{P(u,v)\cdot M_{f,\varphi}(u,v)\Big\} \qquad (6)$$

2.2 Discrete Gabor Decomposition

It is convenient for the decomposition of the Fourier spectrum to define two characteristics of the Gabor filters: the half-peak bandwidth B (in octaves) and the orientation bandwidth Ω (in radians) [11, 4]

$$B = \log_2\left(\frac{\pi F\sigma\lambda + \sqrt{\frac{\ln 2}{2}}}{\pi F\sigma\lambda - \sqrt{\frac{\ln 2}{2}}}\right),\ \Omega = 2\tan^{-1}\left(\frac{\sqrt{\frac{\ln 2}{2}}}{\pi\sigma\lambda}\right)$$

Hence, a given B and Ω determine the variance σ and the ratio λ. The multiplicative connection of F and σ to the constant B induce filters with low frequencies to show wider spatial extention and vice versa. Therefore, choosing $R = \log N/2$ center frequencies which are one octave apart (in cycles per image size)

$$2^0\sqrt{2}, 2^1\sqrt{2}, 2^2\sqrt{2}, \ldots, \frac{N}{4}\sqrt{2}$$

and ω orientations, $\Omega = 2\pi/\omega$, a dense filter bank with elliptical filters touching at their half-peak frequency is generated spanning the Fourier plane. Figure 1 shows the filter bank for $\omega = 6$ and $R = 4$.

For computer based image processing these continuous filters have to be transferred into the discrete pixel domain. Since the filters are not bandlimited, aliasing cannot be avoided. Bovic [11] studied the effects of discretizing filters and gave conditions to adequate sampling densities dependent on f to minimize aliasing effects. Low aliasing is achieved by $f_s > 5\cdot f$ with f_s denoting the sampling frequency. Hence, the highest frequencies should be excluded from the feature generation process.

2.3 Grayscale Gabor Features

The textural measures result from the Gabor decomposition of the image into the spatial/frequency domain $g(x,y)$ (6), which is an image of complex vectors at each pixel position. The complex values can be splitted into magnitude and phase difference [11], but in our experiments only the magnitudes were used for recognition. Because of the symmetry of the Fourier spectrum using real valued input, only the half plane needs is considered. The image features are calculated by summing up the squared filter outputs over the spatial coordinates x and y

$$G_{f,\varphi} = \sum_{x,y} g^2_{f,\varphi}(x,y) \qquad (7)$$

3 Color Gabor Filters

Beside the separate processing of the color bands and the opponent Gabor features of Jain [1] new features based on hue and saturation are introduced.

3.1 Unichrome Features

Unichrome Gabor features are the straight forward way to deal with color images. The features are calculated independently on each color band. The unichrome color feature for spectral band i, center frequency f and orientation φ is defined by

$$U_{i,f,\varphi} = \sum_{x,y} g^2_{i,f,\varphi}(x,y) \qquad (8)$$

For each color band this decomposition can be used for a wavelength specific classification. By concatenation of the feature vectors the full color information can be used (Fig. 2). However, these RGB-features do not utilize the correlation between the color bands.

3.2 Opponent Color Features

The opponent Gabor features [1] are based on the opponent process theory of human color vision. The receptive fields in the retina as a pattern of photoreceptors show spatial and chromatic antagonisms. If one class of photoreceptors in the center is excited by a light stimulus, the opposite photoreceptors in

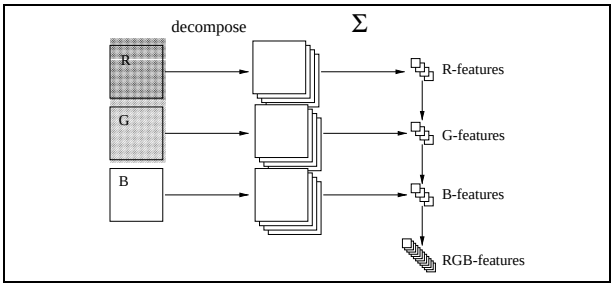

Figure 2: Unichrome R, G and B features and concatenated to RGB features.

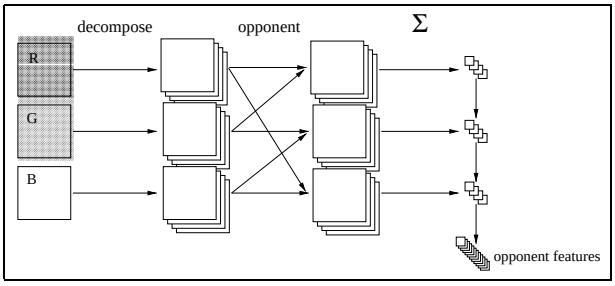

Figure 3: Gabor features by multiplication and normalization of unichrome features based on the opponent theory of human color vision.

the surrounding are inhibited (and vice versa). To integrate this theory into the calculation of Gabor features, the different photoreceptor classes and the spatial relationships are identified with the spectral bands and the neighboring center frequencies, respectively. Therefore, opponent features can be defined by the energy of the difference of two normalized Gabor filtered color bands i and j with fixed orientation and fixed ($f' = f$) or neighboring ($f' = 2f$) center frequencies

$$\sum_{x,y} \left(\frac{g_{i,f,\varphi}(x,y)}{U_{i,f,\varphi}} - \frac{g_{j,f',\varphi}(x,y)}{U_{j,f',\varphi}} \right)^2$$

By removing the redundant information for classification purposes the opponent Gabor features $O_{i,j,f,f',\varphi}$ (Fig. 3) as the normalized cross-correlation between $g_{i,f,\varphi}(x,y)$ and $g_{j,f',\varphi}(x,y)$,$i \neq j$, are received

$$O_{i,j,f,f',\varphi} = \sum_{x,y} \frac{g_{i,f,\varphi}(x,y) g_{j,f',\varphi}(x,y)}{U_{i,f,\varphi} U_{j,f',\varphi}} \qquad (9)$$

For two given bands and $f' = 2f$ there exists $(R-1) \cdot \omega$ features whereas $R \cdot \omega$ features for $f = f'$ are extracted.

3.3 Complex Color Features

The correlation of information between the spectral bands is not integrated in the RGB–features whereas the opponent features handle it as a postprocessing step after the Gabor filtering. The following approach of complex color features combines the color bands previous to the filtering by using the hsv-colorspace.

3.3.1 Color in Complex Representation

The HSV-colorspace is a non-linear transform of the RGB-cube. It is widely used in the field of color vision

$$\begin{aligned} H &= \arctan \frac{\sqrt{3}(G-B)}{(R-G)+(R-B)} \\ S &= 1 - \frac{min\{R,G,B\}}{V} \\ V &= \frac{R+G+B}{3} \end{aligned} \qquad (10)$$

The chromatic components hue, saturation and value correspond closely with the categories of human color perception. One disadvantage are labile values near zero saturation and a singularity at $S = 0$. Therefore the HSV-space should only be used on images with saturated colors. Another problem arises if the Fourier transform is applied on the hue channel. Hue is an angular coordinate which is stored as a scalar value. This implies high frequencies for only soft color changes between red and magenta. To overcome this problem a complex representation for color can be defined [9]

$$b(x,y) = S(x,y) \cdot e^{iH(x,y)} \qquad (11)$$

In this representation saturation is interpretated as magnitude and hue as phase of a complex value b. The value channel is not included. The weighting of

low saturated colors is low, which enables the handling of the described unstability problem. The complex representation (11) is basis for a HSV based Fourier transform as well as for Gabor features of color images. Note that the Fourier spectrum is not symmetric for complex input. Therefore, the entire Fourier plane is used for feature extraction.

3.3.2 Gabor Features for Complex Represented Color

The calculation of the complex color Gabor features is similar to that of unichrome Gabor features, because the combination of the color bands into the complex valued image $b(x, y)$ is done before the filtering (Fig. 4)

$$C_{f,\varphi} = \sum_{x,y} \left(\mathrm{FFT}^{-1} \left\{ B(u,v) \cdot M_{f,\varphi}(u,v) \right\} \right)^2 \quad (12)$$

If the intensity is a discriminatory feature of the texture, these features can be combined with the grayscale features $G_{f,\varphi}$.

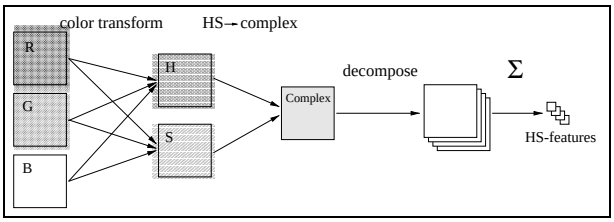

Figure 4: Gabor features after color transformation in complex valued image based on the HSV-colorspace.

4 Experimental Evaluation

From the VisTex[1] database the same thirty images of natural scenes as in [6] were selected (Fig. 5). Each image was subdivided into 64 disjunct 64×64 subimages to generate 1920 images of 30 classes. Seven experiments were done with the above described features, each with Gabor decomposition of 5 center frequencies and 6 orientations (3 for symmetric Fourier planes): 16 grayscale features ($5 \cdot 3$+direct current), 16 unichrome R-, G- and B-features, respectively, 46 concatenated RGB-features ($3 \cdot 15$+DC), 31 HS-features for hue and saturation ($5 \cdot 6$+DC) and 82 opponent color features ($3(3 \cdot 4 + 3 \cdot 5)$+DC). For classification the image set was divided into two disjunct sets of 15 images for each class (chosen by random) for training and testing, respectively. A 5-Nearest-Neighbor classifier was employed.

[1] ftp: whitechapel.media.mit.edu

Figure 5: 30 classes: Bark0, Bark4, Bark6, Bark8, Bark9, Brick1, Brick4, Brick5, Fabric0, Fabric4, Fabric7, Fabric9, Fabric11, Fabric13, Fabric16, Fabric17, Fabric18, Food0, Food2, Food5, Food8, Grass1, Sand0, Stone4, Tile1, Tile3, Tile7, Water6, Wood1, Wood2 (left/right, top/bottom).

5 Results

In our experiments (results in Table 1) the opponent features result worst, whereas the new HS-features and the RGB features perform best and raise the classification rate of the grayscale features. Note that the HS-representation is more compact than RGB.

The classification rates show that the texture of some images is charakterized well enough by the inten-

sitiy values (*Fabric, Sand, Stone, Water*), whereas some show additional color information (*Bark, Food, Wood*). These results reconform the observations of WOUWER [6]. The worst classification results for the image *Wood1*, which is explainable by the bad reprensentation of the texture by a small subimage. Remarkably good results were achieved for *Food0* and *Food2*, although these two images are very similar. Here the HS-features provide the best results.

Features	gray	R	G	B	RGB	opp	hs
Bark	88	89	83	88	91	58	**92**
Brick	91	93	76	90	**96**	48	89
Fabric	**99**	**99**	98	97	**99**	69	**99**
Food	77	81	84	95	86	67	**98**
Grass	94	**97**	94	91	**97**	16	91
Sand	**100**	**100**	**100**	**100**	**100**	78	**100**
Stone	**97**	**97**	**97**	**97**	**97**	19	94
Tile	78	78	80	76	**83**	81	70
Water	**100**	**100**	97	97	**100**	44	**100**
Wood	67	69	70	70	73	55	**81**
$\sum$	89	90	87	90	**92**	61	**92**

Table 1: Classification results in percent. The last row shows the overall performance of the feature sets.

6 Discussion

It is astonishing that in most cases the combined RGB features showed better results than the best features of a single color band. Especially the worst classes (*Food*, *Wood*) of the grayscale features can be enhanced significantly. Although some of the textures seem to be nearly monochrome, the color features RGB and HS perform at least as good as the grayscale features. This is clear for RGB where the intensity information is inherent, but it is noteworthy for the HS-features where the value channel is not used. Both RGB as well as HS-features show good results over the whole dataset, whereas the dimension of the HSV-featurespace is markedly reduced to two third of that of RGB.

7 Conclusion

In this paper complex hue/saturation images were introduced for feature extraction of color textures using Gabor filters. This enables the usage of the HSV-colorspace in this field for the first time. The performance of the new features is compared with other methods dealing with color and/or grayscale information in the field of Gabor transform. For this purpose several classification experiments with 30 natural colored texture images were done. The results encourage the usage of color information for texture classification. This can be done in the RGB- as well as in the HSV-colorspace. Further research will focus on efficiently reducing the number of features without decreasing the classification performance significantly.

References

[1] Jain AK, Healey G: A Multiscale Representation Including Opponent Color Features for Texture Recognition, *IEEE Trans. IP* 7, 1, 124-128, 1998.

[2] Derin H, Cole WS: Segmentation of Textured Images Using Gibbs Random Fields, *CVGIP* 35, 72-98, 1986.

[3] Haralick RM, Shanmugam K, Dinstein I: Textural Features for Image Classification, *IEEE Trans. SMC* 3, 610-621, 1973.

[4] Jain AK, Farrokhnia F: Unsupervised Texture Segmentation using Gabor Filters, *Pattern Recognition* 24, 12, 1167-1186, 1991.

[5] Chang T, Kuo CCJ: Tree-Structured Wavelet Transform for Textured Image Segmentation, *Proc. SPIE* 1770, 394-405, 1992.

[6] Van de Wouwer G, Scheunders P, Livens S, Van Dyck D: Wavelet Correlation Signatures for Color Texture Characerization, *Pattern Recognition* 32, 443-451, 1999.

[7] Palm C, Metzler V, Mohan B, Dieker O, Lehmann T, Spitzer K: Co-Occurrence Matrizen zur Texturklassifikation in Vektorbildern, In: Evers H, Glombitza G, Lehmann T, Meinzer H-P: Bildverarbeitung für die Medizin 1999, Springer Verlag, Berlin, 367-371, 1999.

[8] Lakmann R, Priese L: A reduced covariance color texture model for micro-textures, In: Proceedings 10th Scandinavian Conference on Image Analysis, Lappeenranta, Finland, 947-953, 1997.

[9] Frey H: Digitale Bildverarbeitung in Farbräumen, PhD thesis, Technical University of Munich, 1988.

[10] Gabor D: Theory of Communication, *Journal of IEE* 93, 429-457, 1946.

[11] Bovik AC, Clark M, Geisler WS: Multichannel Texture Analysis Using Localized Spatial Filters, *IEEE Trans. PAMI* 12, 1, 55-73, 1990.